Runaway electron generation in tokamak disruptions

P. Helander[1], F. Andersson[2], L.-G. Eriksson[3], T. Fülöp[2], H. Smith[2], D. Anderson[2], M. Lisak[2]

[1]EURATOM/UKAEA Fusion Association, Culham Science Centre, Abingdon, UK
[2]Dept. of Electromagnetics, Chalmers University of Technology, Göteborg, Sweden
[3]Association EURATOM-CEA sur la Fusion, CEA Cadarache, France

E-mail contact of main author: per.helander@ukaea.org.uk

Abstract. The time evolution of the plasma current during a tokamak disruption is calculated by solving the equations for runaway electron production simultaneously with the induction equation for the toroidal electric field. The resistive diffusion time in a post-disruption plasma is typically comparable to the runaway avalanche growth time. Accordingly, the toroidal electric field induced after the thermal quench of a disruption diffuses radially through the plasma at the same time as it accelerates runaway electrons, which in turn back-react on the electric field. When these processes are accounted for in a self-consistent way, it is found that (1) the efficiency and time scale of runaway generation agrees with JET experiments; (2) the runaway current profile typically becomes more peaked than the pre-disruption current profile; and (3) can easily become radially filamented. It is also shown that higher runaway electron generation is expected if the thermal quench is sufficiently fast.

1. Model equations

Tokamak discharges are often terminated by plasma disruptions causing enormous mechanical and thermal loads on the vessel. Of particular concern in large tokamaks is the acceleration of "runaway" electrons to relativistic energies, which may seriously damage the first wall on impact. Until now, despite several decades of theoretical and experimental research on runaway electrons, there has been little quantitative understanding of their production and behaviour in tokamak disruptions. Runaway electron theory has traditionally focused on the physical mechanisms producing the fast electrons and how to calculate their efficiency, but relatively little effort has been devoted to analyzing the consequences for what actually happens in a tokamak disruption. This is the topic of the present work, where the post-disruption runaway current profile is calculated from pre-disruption plasma parameters. For this calculation it is important to treat the toroidal electric field in a consistent manner. This field is initially induced by the drop in electron temperature during the thermal quench of the disruption, leading to a dramatic increase in the plasma resistivity. The electric field accelerates runaways, whose rising current limits the further growth of the field. Since the runaways thus modify the electric field responsible for their own creation, the system is nonlinear and exhibits mathematically interesting behaviour. Its complexity is further enhanced by the fact that the growth rate of the runaway population is comparable to the resistive

diffusion rate of the electric field. This field thus diffuses through the plasma whilst generating the runaway current and being modified thereby.

In our analysis [1], we do not consider the very first stage of a disruption, which is characterised by MHD instability, but instead focus on the subsequent stage, in which the plasma has regained axisymmetry, cools down, and the current evolves from its Ohmic (or non-inductive) pre-disruption state to one where all the remaining current is carried by runaway electrons. The production of runaways takes about 5-10 ms in JET and is the result of two distinct physical processes: primary (Dreicer) generation and secondary (avalanche) generation. The former is caused by a diffusion process in velocity space and generates runaways (in a pure plasma) at the rate [2]

$$\dot{n}_r^I = \frac{n_e}{\tau}\left(\frac{m_e c^2}{2T_e}\right)^{3/2}\left(\frac{E_D}{E_\parallel}\right)^{3/8}\exp\left(-\frac{E_D}{4E_\parallel}-\sqrt{\frac{2E_D}{E_\parallel}}\right), \tag{1}$$

where $\tau = 4\pi\epsilon_0^2 m_e^2 c^3/n_e e^4 \ln\Lambda$ is the relativistic electron collision time, $E_\parallel$ the parallel electric field, and $E_D = m_e^2 c^3/e\tau T_e$ the Dreicer field. Secondary runaway production is caused by collisions at close range between existing runaway electrons and thermal ones and produces new runaways at the rate [3]

$$\dot{n}_r^{II} \simeq \left(\frac{\pi}{2}\right)^{1/2}\frac{n_r(E_\parallel/E_c-1)}{3\tau\ln\Lambda},$$

where $E_c = m_e c/e\tau$ is the relativistic cut-off field below which no runaway generation can occur [4]. Adding these equations and writing the result in terms of dimensionless variables gives

$$\partial_t n = F(E,x,t) + n(E-\hat{n}), \tag{2}$$

where $\hat{n} = n_e(x)/n_e(0)$, $n(x,t) = n_r/n_{r0}$, $x = r/a$ is the normalised radius, $n_{r0} = j_0/ec$ and j_0 is the pre-disruption current density on axis. Furthermore $E = E_\parallel/E_c(0)$, time has been normalised to $3(2/\pi)^{1/2}\tau_0\ln\Lambda$, with $\tau_0 = \tau(x=0)$, and we have written

$$F(E,x,t) = \frac{3\ln\Lambda n_e(0)\hat{n}^{19/8}}{2\pi^{1/2}n_{r0}u^{15/4}E^{3/8}}\exp\left(-\frac{1}{4u^2E}-\sqrt{\frac{2}{u^2E}}\right), \tag{3}$$

with $u^2(x,t) = T_e(x,t)/m_e c^2 \ll 1$. The electric field in these equations is governed by the induction equation, $\nabla^2 E_\parallel = \mu_0 \partial j_\parallel/\partial t$, where $j_\parallel$ is the current density. The simplest way to close the system is to assume that the current consists of two parts: a thermal current governed by (the neoclassical) Ohm's law, and a runaway current carried by electrons all moving at the speed of light, $j_\parallel(x,t) = \sigma_\parallel(x,t)E_\parallel(x,t) + n_r(x,t)ec$. This neglects the time required to accelerate a newly generated runaway electron to c and is accurate if most runaways are created by the secondary mechanism since the acceleration time $t_{\rm acc} \sim m_e c/eE_\parallel = \tau/E$ is then shorter than the avalanche growth time $t_{\rm av} \sim \tau\ln\Lambda/E$. In a plasma with circular cross section the equation for the electric field thus becomes

$$\partial_t(\sigma E + n) = \alpha^{-1}\nabla^2 E, \tag{4}$$

where $\nabla^2(\cdots) = x^{-1}\partial_x[x\partial_x(\cdots)]$, $\sigma(x,t) = m_e\sigma_\parallel/n_{r0}e^2\tau_0$, and

$$\alpha = \frac{(2\pi)^{3/2}}{3\ln\Lambda}\frac{j_0 a^2}{I_A},$$

with $I_A = 4\pi m_e c/\mu_0 e$ the Alfvén current. The boundary condition on the electric field is $E(1,t) = 0$ if the plasma is surrounded by a perfectly conducting wall at $x = 1$. If the wall is instead at $x = b > 1$, with a vacuum region in the region $1 < x < b$, then the boundary condition at $x = 1$ is obtained by matching to the vacuum solution $E(x,t) \sim \ln(b/x)$, giving $E(1,t) + (\ln b)\partial_x E(1,t) = 0$.

2. Disruption dynamics

Equations (2) and (4) govern the evolution of the normalized runaway current density $n(x,t)$ and electric field $E(x,t)$, if $T_e(x,t)$ and hence $\sigma(x,t)$ are given. The thermal quench is described by letting T_e drop rapidly, typically as

$$T_e(x,t) = T_1(x) + [T_0(x) - T_1(x)]e^{-t/t_0}.$$

We have solved Eqs. (2) and (4) numerically for a large number of cases with JET-like parameters, and generally find good agreement with experimental observations – sometimes within considerable uncertainties due to the violent nature of the disruption. The fraction of the pre-disruption current that is converted to runaway electrons is typically around 1/2, the time scale for runaway generation about 10 ms, and the edge loop voltage of the order of 100 V. These results depend to some extent on the post-disruption temperature, which is unknown but has been conjectured to be around 10 eV from indirect evidence [5] and is therefore chosen accordingly in the simulations.

Figure 1 shows an example of such a simulation where the paramaters are chosen to match a recent JET disruption experiment (pulse 63133): $T_0 = (1 - 0.9x^2)^2 \cdot 3.1$ keV, $T_1 = 10$ eV, $n_e(x,t) = (1-0.9x^2)^{2/3} g(t) \cdot 2.8 \cdot 10^{19}$ m^{-3}, $g(t) = e^{-(t/t_0)^2} + 1.96e^{-(t-t_1)^2/t_2^2}$, $t_0 = 0.5$ ms, $t_1 = 10$ ms, $t_2 = 3.2$ ms, $a = 1$ m. The initial plasma current, $I_0 = 1.9$ MA, is converted to a runaway current of 1.3 MA in the simulation (1.1 MA in the experiment), with 3/8 of the runaways produced by the Dreicer mechanism and the remaining 5/8 by the secondary avalanche. These numbers are typical: in most JET simulations somewhat more than half the runaways are secondaries. A further feature seen in the simulation is that the post-disruption current, which is carried by runaway electrons, has a more peaked profile than the pre-disruption current. In fact, the current density actually increases in the centre of the discharge although the total current falls. This may have implications for the MHD stability of the post-disruption plasma. The reason for the peaking of the current is that runaway generation is most efficient in the centre of the plasma, so that the growth of the toroidal electric field is first limited there. Some time after the thermal quench, the electric field therefore has an off-axis maximum, see Fig. 2, causing inward diffusion of the field and hence increased runaway production near the magnetic axis. Notice in Fig. 2 that the electric field is much larger inside the plasma than at the edge.

The agreement between theory and experiment in JET gives confidence that the model can be used for ITER predictions. The calculated conversion of Ohmic plasma current to runaways is calculated to be be higher in ITER than in JET; the runaways typically carry about 3/4 of the pre-disruption current. The reason for this is that the efficiency

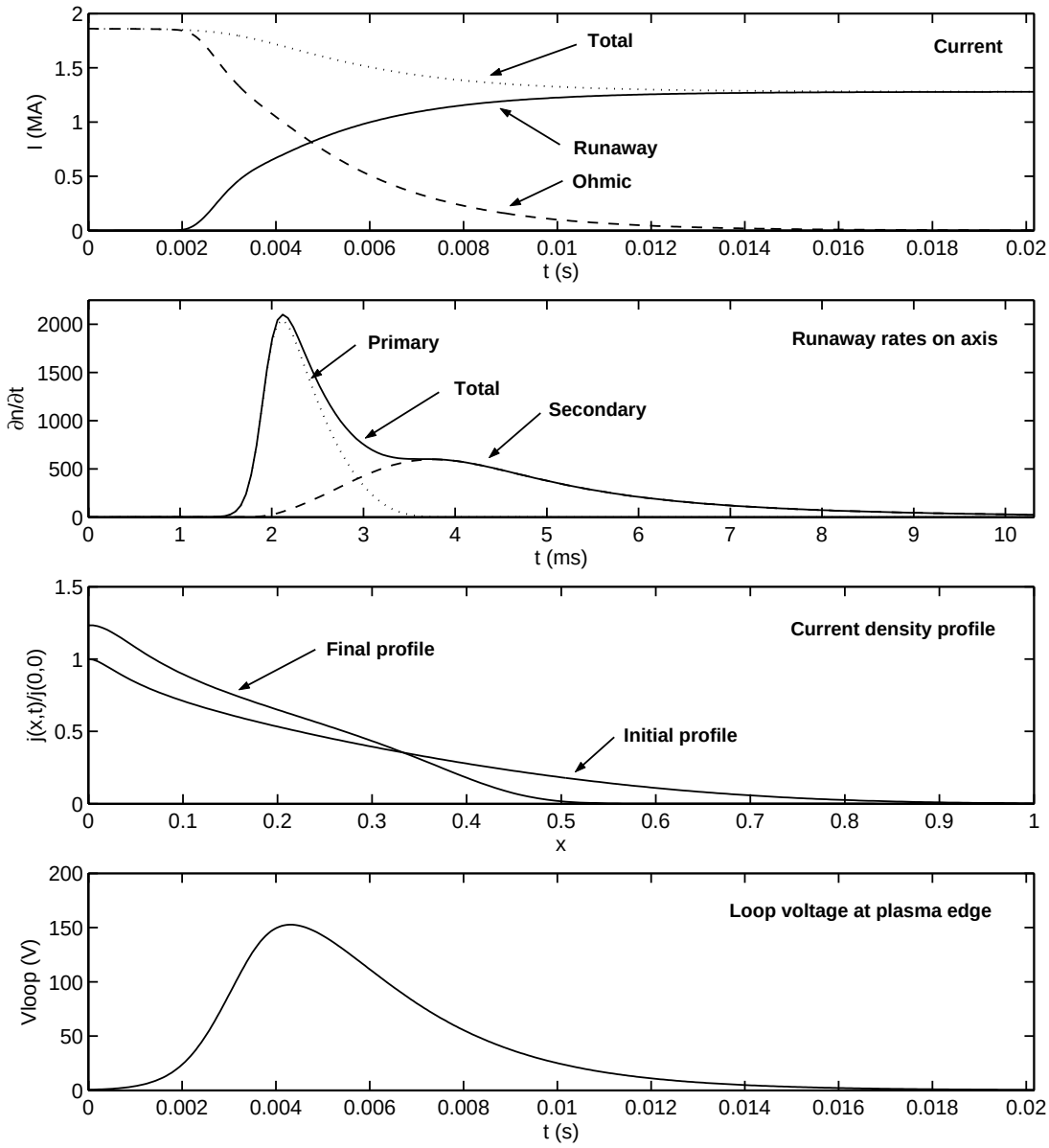

Figure 1: *Simulation of a recent JET disruption (pulse 63133).*

of the runaway avalanche increases with plasma current [3]. Secondary production is by far the dominant generation mechanism in ITER. For both JET and ITER, the results from solving Eqs. (2) and (4) agree well with full Fokker-Planck simulations of the fast electron population carried out with the ARENA code, which also calculates the toroidal electric field self-consistently [7].

The outcome of the numerical simulations can be understood analytically by noting that the primary production of runaways is very swift, see Fig. 1. The role of primary production is mainly to provide a "seed" for the secondary avalanche. After some short time, t_*, most subsequent runaway production will occur by the secondary mechanism so that F can be neglected in Eq. (2). Assuming $E \gg 1$, eliminating $E = \partial_t \ln n$ from Eq. (4) and integrating with respect to time then gives

$$\sigma \partial_t N = j_* - e^N - \alpha^{-1} \nabla^2 (N_* - N)$$

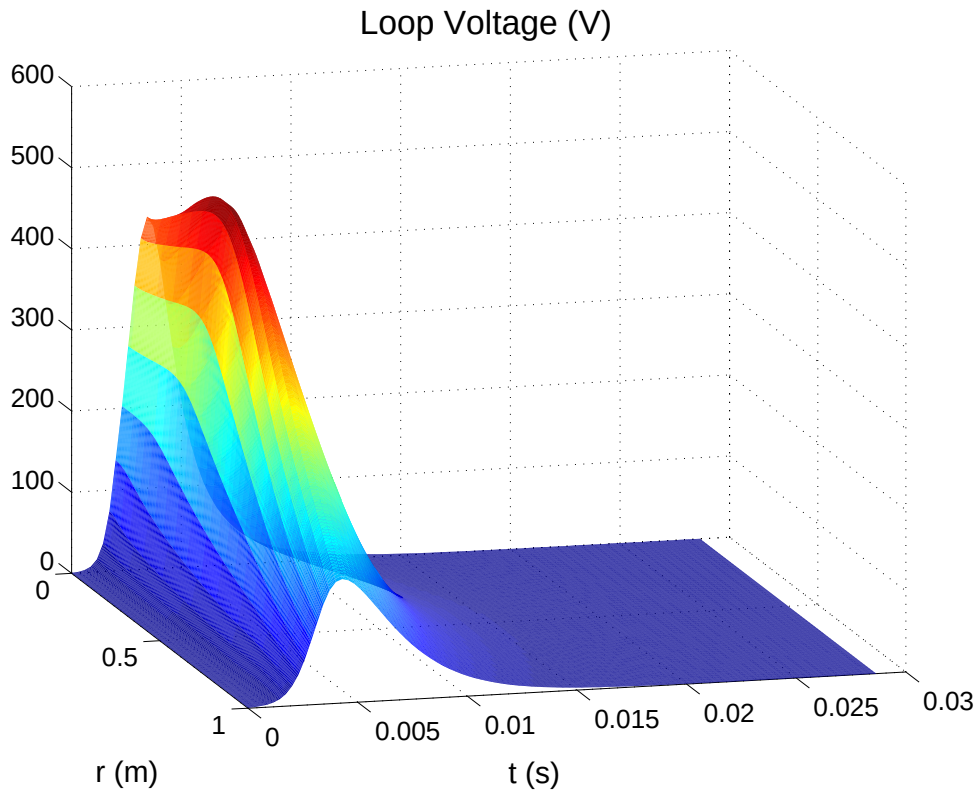

Figure 2: *Loop voltage for the simulation shown in Fig. 1.*

where $N(x,t) = \ln n(x,t)$, $N_*(x) = \ln n(x,t_*)$ and $j_*(x) = \sigma(x,t_*)E(x,t_*) + n(x,t_*)$ is the total current at $t = t_*$. From this partial differential equation for the runaway density an *ordinary* differential equation for the final state $N(x,\infty)$ follows by setting $\partial_t N = 0$,

$$e^N = j_* - \alpha^{-1}\nabla^2(N_* - N). \tag{5}$$

This equation allows the final runaway current profile to be determined if the runaway seed from primary generation, $N_*(x)$, and the total current profile $j_*(x)$ at $t = t_*$ are known. When secondary production dominates, the time t_* occurs very early and j_* is approximately equal to the initial current profile.

In the limit $\alpha \to \infty$, Eq. (5) implies that all the current j_* is converted to runaways. In this limit, the skin time is so large that no electric field can escape from the plasma and all the field is thus available for runaway production. Indeed, when $\alpha \to \infty$ Eq. (2) reduces to

$$\frac{\partial n}{\partial t} = \frac{n(j_* - n)}{\sigma}$$

for $t > t_*$ and $E \gg 1$, and hence

$$n(x,t) = j_*(x)\left[1 + (j_*(x)e^{-N_*(x)} - 1)\exp\left(-j_*(x)\int_{t_*}^{t}\frac{dt'}{\sigma(x,t')}\right)\right]^{-1}.$$

Hence all the seed current $j_*(x)$ is replaced by runaways on a time scale set by the avalanche growth time and the cooling time.

In JET and ITER $\alpha \gtrsim 10^2$, and it is therefore surprising at first sight that even more runaways are not created than suggested by the simulations discussed above. The mathematical reason for this is that Eq. (5) contains another large term, namely, $\nabla^2 N_*$, which is large since primary production is exceedingly sensitive to the electron temperature, making $N_*(x)$ highly peaked in the centre of the discharge. Indeed, in the limit of a fast thermal quench and small seed from primary production, one can show that [1]

$$\nabla^2 N_* \simeq -\nabla^2 \left(E_D/4E_\parallel + \sqrt{2E_D/E_\parallel} \right) \gg 1.$$

It follows from Eq. (5) that the final current is always smaller than the initial current, i.e., the runaway current can never exceed the pre-disruption current, as always observed in experiments. This conclusion follows by taking the first moment of Eq. (5), giving

$$\int_0^1 (j_* - e^N) x dx = -\alpha^{-1} \left. \frac{d(N - N_*)}{dx} \right|_{x=1} \geq 0,$$

since $N(x) \geq N_*(x)$ for all x and we have assumed that there are no runaways on the boundary.

Another immediate consequence of Eq. (5) is that any radial fluctuations in the seed profile $N_*(x)$ are "inherited" by the final runaway current profile $N(x)$. Because the Dreicer function (3) depends sensitively on the electron density and temperature, it is likely that $N_*(x)$ exhibits rapid radial variations. These variations are reflected in the final current profile even if most runaways are eventually generated by the secondary mechanism. This is because the highest derivative in Eq. (5) operates on $N - N_*$, so that this difference cannot vary suddenly. Linearisation of Eq. (5) shows that sufficiently fine-scale fluctuations, of wave-length $\Delta x \lesssim \alpha^{-1/2}$, are similar in $N_*(x)$ and $N(x)$. Figure 2 illustrates this effect by showing the current profile in a simulation where all parameters are chosen as in Fig. 1 except the cooling time t_0, which varies sinusoidally with radius as $t_0 = [1 + 0.25 \sin(20\pi x)] \cdot 0.5$ ms.

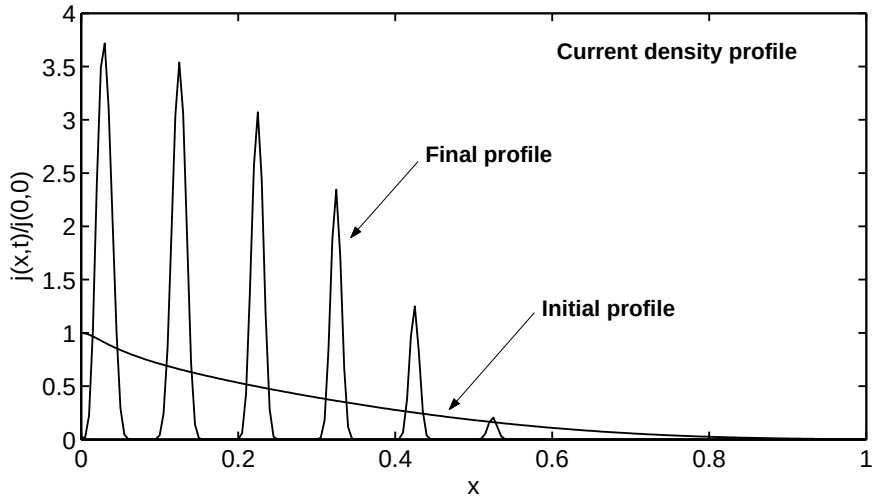

Figure 3: *Current profiles from a simulation with the same parameters as in Fig 1, but with t_0 varying sinusoidally by $\pm 25\%$.*

3. Effect of finite cooling time

The conventional expression (1) for primary runaway generation was derived assuming quasi-stationary conditions [2]. Although the number of runaways increases with time, the bulk of the electron distribution function is assumed to be in a steady state. In a tokamak disruption, this assumption requires the characteristic time in which the plasma cools down to be much longer than the collision time for electrons near the runaway threshold energy. In JET, where the thermal quench is faster than 1 ms, this requirement is often only marginally satisfied, at best. In ITER it may fail altogether depending on the temporal structure of the thermal quench (in particular, the delay between its first and second stages). This should make primary runaway generation much more efficient since incompletely thermalised electrons in the tail of the hot, pre-disruption distribution can be accelerated relatively easily. This has been noticed in numerical simulations of disruption mitigation by "killer pellets" [8,9]. On the other hand, if the magnetic field is ergodised and connects to the wall, then the high-energy electron population is depleted, which should result in lower runaway production.

An analytical understanding of runaway generation in a cooling plasma can be gained by solving the kinetic equation for suprathermal electrons colliding with a Maxwellian with decreasing temperature [7]. If the velocity v is normalised to the instantaneous thermal speed $v_{Te} = [2T_e(t)/m_e]^{1/2}$ and the distribution function is written as $f(v,t) = n_e\tilde{f}(v,t)/\pi^{3/2}v_{Te}^3$, then $\tilde{f}$ satisfies

$$\frac{\partial\tilde{f}}{\partial s} + \delta\left(3\tilde{f} + v\frac{\partial\tilde{f}}{\partial v}\right) = \frac{1}{v^2}\frac{\partial}{\partial v}\left(\tilde{f} + \frac{1}{2v}\frac{\partial\tilde{f}}{\partial v}\right).$$

Here the increment of the time variable s is normalised to the instantaneous collision time, $ds/dt = \nu(t)$ with $\nu(t) = (c/v_{Te}^3)/\tau$, and $\delta = -(1/2)d\ln T_e/ds$ measures the cooling rate. For simplicity, the density is kept constant and the electric field is ignored. When the parameter δ is constant and small, so that $T_e(t) = T_0(1 - t/t_0)^{2/3}$ with $t_0^{-1} = 3\delta\nu(0)$, the kinetic equation can be solved by matched asymptotic expansion. The result is that f approaches a self-similar form

$$\tilde{f}(y,t) = \begin{cases} \exp\left[-\frac{1}{\delta^{2/3}}\left(y^2 - \frac{2y^5}{5}\right)\right], & y < 1 \\ \frac{1}{2}\exp\left[\frac{3}{\delta^{2/3}}\left((y-1)^2 - \frac{1}{5}\right)\right]\mathrm{erfc}\left(\frac{\sqrt{3}(y-1)}{\delta^{1/3}}\right), & y - 1 \sim \delta^{1/3} \\ \frac{\delta^{1/3}}{2}\left(\frac{3}{\pi}\right)^{1/2}\exp\left(-\frac{3}{5\delta^{2/3}}\right)\frac{1}{y^3-1}, & y > 1 \end{cases} \tag{6}$$

where $y = v\delta^{1/3}$, indicating the development of a high-energy tail $f \sim v^{-3}$ in the distribution function.

In a disruption, the electric field $E_\parallel$ initially increases in proportion to $T_e^{-3/2}$. The size of the runaway population created by this field can be estimated as the number of electrons above the (normalised) critical runaway velocity $v_c = \sqrt{E_D/2E_\parallel}$. This velocity falls in the tail ($y > 1$) of Eq. (6) if

$$\nu(0)t_0 < \frac{1}{3}\left(\frac{E_D}{2E_\parallel}\right)_{T=T_1}^{3/2}, \tag{7}$$

where the right-hand side is evaluated at the end of the thermal quench, when the temperature has fallen to $T_1 \ll T_0$, and can be written as [10]

$$\left.\frac{E_D}{2E_\parallel}\right|_{T=T_1} = \frac{3\mu_0 eqRn_e}{B}\sqrt{\frac{\pi T_1}{8m_e}}.$$

If the condition (7) is satisfied, then the thermal quench is so quick that Dreicer runaway production is significantly more efficient than suggested by the usual formula (1). This may well be the case in JET and seems even more likely in ITER.

This work was funded by the UK Engineering and Physical Sciences Research Council, and by EURATOM under association contracts with Sweden, France and UK.

[1] ERIKSSON, L-G., HELANDER, P., ANDERSSON, F., ANDERSON, D., LISAK, M., Phys. Rev. Lett. **92** (2004) 205004.

[2] GUREVICH, A.V., Sov. Phys. JETP **12** (1961) 904; KRUSKAL, M.D., BERNSTEIN, I.B., PPPL Report MATT-Q-20 (1962) 174.

[3] ROSENBLUTH, M.N., PUTVINSKI, S.V, Nucl. Fusion **37** (1997) 1355.

[4] CONNOR, J.W., HASTIE, R.J., Nucl. Fusion **15** (1975) 415.

[5] WESSON, J.A., et al., Nucl. Fusion **29** (1989) 641.

[6] ERIKSSON, L-G., HELANDER, P., Comp. Phys. Comm. **154** (2003) 175.

[7] HELANDER, P., H. SMITH, T. FÜLÖP, ERIKSSON, L-G., to appear in Phys. Plasmas (2004).

[8] CHIU, S.C., ROSENBLUTH, M.N., HARVEY, R.W., CHAN, V.S., Nucl. Fusion **38** (1998) 1711.

[9] HARVEY, R.W. et al., Phys. Plasmas **7** (2000) 4590.

[10] HELANDER, P., ERIKSSON, L-G., ANDERSSON, F., Plasma Phys. Contr. Fusion **44** (2002) B247.